Separation Science and Technology
Publication details, including instructions for authors and subscription information:
http://www.informaworld.com/smpp/title~content=t713708471

The Depletion of Aqueous Nitrous Acid in Packed Towers

Douglas B. Crawford[a]; Robert M. Counce[bcd]
[a] Chemical Engineering Department, University of Tennessee Knoxville, Tennessee [b] Chemical Engineering Department, The University of Tennessee, Knoxville, Tennessee [c] Chemical Technology Division, Oak Ridge National Laboratory, Oak Ridge, Tennessee [d] Martin Marietta Energy Systems, Inc.,

To cite this Article Crawford, Douglas B. and Counce, Robert M.(1988) 'The Depletion of Aqueous Nitrous Acid in Packed Towers', Separation Science and Technology, 23: 12, 1573 — 1594
To link to this Article: DOI: 10.1080/01496398808075650
URL: http://dx.doi.org/10.1080/01496398808075650

SEPARATION SCIENCE AND TECHNOLOGY, 23(12&13), pp. 1573-1594, 1988

THE DEPLETION OF AQUEOUS NITROUS ACID IN PACKED TOWERS[a]

Douglas B. Crawford
Chemical Engineering Department
University of Tennessee
Knoxville, Tennessee 37996

Robert M. Counce[b]
Chemical Technology Division
Oak Ridge National Laboratory[c]
Oak Ridge, Tennessee 37831-6044

ABSTRACT

The depletion of aqueous nitrous acid was studied at 298 K and at slightly greater than atmospheric pressure. Solutions containing nitrous and nitric acids were contacted with nitrogen in towers packed with 6- and 13-mm Intalox saddles. The results indicate the existence of two depletion mechanisms for the conditions studied – liquid-phase decomposition and direct desorption of nitrous acid. Models based on mass-transfer and chemical-kinetic information are presented to explain the experimental results.

---

[a]Research sponsored by the Office of Facilities, Fuel Cycle, and Test Programs, U.S. Department of Energy, under Contract No. DE-AC05-84OR21400 with Martin Marietta Energy Systems, Inc. Research also sponsored by the State of Tennessee Center of Excellence for Waste Management, The University of Tennessee, Knoxville, Tennessee.

[b]Address correspondence to Robert M. Counce, Chemical Engineering Department, The University of Tennessee, Knoxville, Tennessee 37996-2200.

[c]Operated by Martin Marietta Energy Systems, Inc., for the U.S. Department of Energy.

INTRODUCTION

The depletion of HNO_2 from aqueous solutions is an integral part of nitrogen oxide absorption from gas streams and is also an important step in the manufacture of certain organic chemicals. The term "depletion" is used because the disappearance of HNO_2 from aqueous solutions involves liquid-phase decomposition and direct desorption phenomena. The purpose of this study was to obtain data on the depletion of HNO_2 at conditions near those encountered in nitrogen oxide scrubbing studies reported separately (1) and to develop a model describing the controlling depletion stoichiometry and associated rate constants based on the best available information on mass-transfer, kinetic and equilibrium constants.

The depletion of HNO_2 from aqueous solutions tends to be heterogeneous due to the volatilization of NO, a highly insoluble decomposition reaction product, and to the desorption of HNO_2 from solution. Experimental results from batch systems tend to focus on the liquid-phase decomposition, whereas experimental results from semibatch or continuous contact systems tend to involve both liquid-phase decomposition and direct desorption.

The best known equation for describing the liquid-phase decomposition of nitrous acid from aqueous solutions is

$$3HNO_2(\ell) \leftrightarrow H^+(\ell) + NO^-{}_3(\ell) + H_2O(\ell) + 2NO(g). \quad (1)$$

This overall equation was developed by Abel and Schmid.(2) Working in an NO atmosphere, in a completely batch system and under conditions of extremely high-liquid-phase mass transfer, this decomposition process is fourth order with respect to aqueous HNO_2.(3) The decomposition sequence is

$$4HNO_2(\ell) \leftrightarrow N_2O_4(\ell) + 2NO(\ell) + 2H_2O(\ell) \ , \quad (2)$$

and

$$N_2O_4(\ell) + H_2O(\ell) \leftrightarrow HNO_2(\ell) + H^+(\ell) + NO_3^-(\ell) \ , \quad (3)$$

with Eq. (3) being the rate-controlling step. The resulting rate expression is

$$-r_{HNO_2} = k_1 \frac{C^4_{HNO_2}}{P^2_{NO}} - k_{-1} C_{HNO_2} C_{H^+} C_{NO_3^-} \ . \quad (4)$$

Because of the reversibility of this decomposition reaction, the rate-controlling process may be linked to the removal of NO from solution,

$$-r_{HNO_2} = \frac{3}{2} k_L a' (C_{NO} - C^*_{NO}) \ . \quad (5)$$

Expressions combining these mass-transfer and kinetic limitations of the decomposition process have been obtained by Andrews and Hanson (4) and Komiyama and Inoue (5) similar to

$$-r_{HNO_2} = \left(\frac{3}{2}\right)^{2/3} \left[\frac{(k_L a')^2 (k_1)}{H_{NO}^2}\right]^{1/3} C_{HNO_2}^{4/3} \quad (6)$$

By working with Abel-Schmid kinetics, the order of the aqueous HNO_2 decomposition reaction can vary from 4/3 predicted by Eq. (6) to 4 predicted by Eq. (4). The Abel-Schmid stoichiometry also stipulates the molar ratio of HNO_3 produced to HNO_2 disappearing from solution to be 1/3. For convenience, this molar ratio is referred to as R*.

Some researchers, however, have found R* to be less than 1/3 in studies into the nonoxidizing depletion of aqueous HNO_2. The value of R*, found by Komiyama and Inoue (5), was about 1/3 in studies with a helium-sparged semibatch contactor; the corresponding depletion order, with respect to HNO_2, in these studies was about 4/3. In further studies, with an agitated nonsparged semibatch gas-liquid contactor, R* decreased with increasing ratios of gas to liquid flow rates; in these studies, the order of the depletion reaction also approached unity, with respect to HNO_2, as the gas rate was increased. This decrease in R* was also noted by Lang and Aunis (6,7) in aqueous HNO_2 depletion studies as the N_2 rate to a sparged gas-liquid contactor was increased; the depletion order in these studies was about 1. The value of R* is also reported by Safin et al., (8) to decrease from 1/3 to zero as the NO content was increased in the N_2 sparge gas of an aqueous HNO_2 mixture. The order of the reaction was reported by Leibmann (9) to decrease from 3 to 1 as aqueous HNO_2 was removed in a N_2-sparged device. These depletion rates generally increase with gas sparge rate and agitation.

The decreasing value of R* suggests that species other than NO can be desorbed during the depletion of HNO_2 from aqueous solutions. The near first-order depletion kinetics associated with results with R* less than 1/3 and its sensitivity to gas rates and agitation suggest that the physical desorption of nitrous acid can occur which produces an R* of 0. Thus, the stoichiometric boundaries for R* are 1/3 and 0 for the nonoxidizing depletion of aqueous HNO_2.

In this study, aqueous solutions of HNO_2 and HNO_3 were contacted with N_2 in towers packed with Intalox saddles. The results indicate the existence of two depletion mechanisms – liquid-phase decomposition and direct desorption of HNO_2. In this study, the liquid-phase decomposition tended to be controlled by liquid-phase resistance with reaction occurring primarily in the bulk liquid region and also to a smaller extent in the liquid-phase mass-transfer film region; the direct desorption tended to be controlled by gas-phase resistances. Two depletion models are presented – a fairly rigorous treatment and a greatly simplified

approach. Both models provide reasonably a priori predictions of the experimental depletion rates and stoichiometry.

THEORY

The experiments described are designed to provide information on the depletion of nitrous acid from aqueous solutions by means of countercurrent flow of gaseous nitrogen in packed columns. The nitrous and nitric acid strengths were less than 0.08 and 0.23 kmol/m^3 in this study. Under these and other experimental conditions, the prevalent liquid-phase species are HNO_2, H^+, NO^-_3, H_2O, and NO.

The important depletion mechanisms in this study were postulated to be the decomposition of nitrous acid in the liquid phase coupled with the desorption of the reaction product NO,

$$3HNO_2(\ell) \leftrightarrow H^+(\ell) + NO_3^-(\ell) + H_2O(\ell) + 2NO(\ell) \ , \tag{7}$$

and

$$NO(\ell) \leftrightarrow NO(g) \ , \tag{8}$$

and the desorption of nitrous acid,

$$HNO_2(\ell) \leftrightarrow HNO_2(g) \ . \tag{9}$$

The relative importance of these two mechanisms is indicated by the molar ratio of nitric acid produced to nitrous acid depleted (R*). This ratio for nonoxidizing conditions is 1/3 for the liquid-phase decomposition route and 0 for the direct desorption route. The total liquid-phase acid concentrations as determined by chemical analysis may be represented by:

$$C_{H^+} = C_{HNO_2} + C_{HNO_3} \ , \tag{10}$$

and thus changes may be represented by

$$\Delta C_{H^+} = \Delta C_{HNO_2} + \Delta C_{HNO_3} \ . \tag{11}$$

The quality R* may be found by a rearrangement as

$$R^* = (-) \frac{\Delta C_{HNO_3}}{\Delta C_{HNO_2}} = 1 - \frac{\Delta C_{H^+}}{\Delta C_{HNO_2}} \ . \tag{12}$$

In the following sections, models are developed for the depletion rate of HNO_2 in the column, Φ_T, where

$$\Phi_T = L\ (C_{HNO_2,in} - C_{HNO_2,out})\ . \tag{13}$$

This depletion rate will have a liquid-phase decomposition component and a direct desorption component.

Model A

Model A is based on the following assumptions: (1) the depletion of aqueous HNO_2 can be described by liquid-phase decomposition of HNO_2 coupled with the desorption of NO and the direct desorption of HNO_2, (2) the gas phase behaves ideally, (3) the liquid phase is at chemical equilibrium when introduced into the column, (4) the column gas and liquid phases behave as a number of continuously stirred tank reactors (CSTRs), and (5) the gas-liquid contact may be modeled with the film theory.

Material balance difference equations allow the HNO_2 decomposition reaction to occur in both the liquid-phase bulk and film regions as well as through direct desorption of HNO_2:

$$L\Delta C_i = \left[\nu_i r_{HNO_2} \varepsilon_L + \nu_i \left(\int_{\delta_L}^{o} r_{HNO_2} dx \right) a + N_i^* a \right] \Delta V\ , \tag{14}$$

for the liquid phase and

$$\frac{G}{RT} \Delta P_i = N_i^*\ a\ \Delta V\ , \tag{15}$$

for the gas phase. The respective concentration and partial-pressure gradients within their respective mass-transfer films are:

$$\frac{dC_i}{dX_L} = \frac{1}{D_i^L} \left[\frac{C_i}{C_T} \left(\sum_j N_j \right) \right] - N_i\ , \tag{16}$$

and

$$\frac{dP_i}{dX_G} = \sum_{j=1} \frac{\pi}{RT\ D_{ij}^G} (P_i N_j - P_j N_i)\ . \tag{17}$$

Reaction within the liquid mass-transfer film is accounted for by:

$$\frac{dN_i}{dX_L} = \nu_i\ r_{HNO_2}\ . \tag{18}$$

These equations constitute a system of first-order ordinary differential equation which may be solved by numerical integration as an initial value problem. The initial conditions are:

$$\text{at } X_L = \delta_L = \frac{D^L_{NO}}{k_{L,NO}} , \quad N_i = N_i^o \text{ and } C_i = C_i^o ;$$

$$\text{at } X_L = X_G = 0 , \quad (N_i^*)_L = (N_i^*)_G \text{ and } P_i^* = K_i C_i^* ;$$

$$\text{at } X_G = \delta_G = \frac{D^G_{HNO_2}}{k_{G,HNO_2} RT} , \quad P_i = P_i^o ;$$

$$\text{at } Z = 0 , \quad P_{NO} = P_{HNO_2} = P_{HNO_3} = P_{H_2O} = 0 \text{ and } P_{N_2} = \pi ;$$

$$\text{at } Z = Z_c , \quad C^o_{NO} = \left[\frac{K_1 (C_{HNO_2})^3}{H^2_{NO}\, C_H C_{NO_3}} \right]^{1/2} . \tag{19}$$

The calculation of Φ_T proceeds with a series of incremental calculations beginning at the bottom of the column; the size of the incremental volume, ΔV, is determined by dividing the gas and liquid phases of the column into a number of CSTRs. The volume is related to the height of the increment by

$$\Delta V = S \Delta Z . \tag{20}$$

The height Z is then related to the total height of the column, Z_c, by

$$\Delta Z = Z_c / B , \tag{21}$$

where B is the number of liquid-phase CSTRs. The number of liquid-phase CSTRs is related to the Peclet number, Pe, by Carberry (10):

$$B = \frac{1}{2} Pe \left(\frac{Z_c}{d_p} \right) . \tag{22}$$

The Peclet number is calculated by a correlation by Otake and Kunugta (11):

$$Pe = 1.9 \, (Re)_L^{1/2} \, (Ga)_L^{-1/3} . \tag{23}$$

The height of the gas-phase CSTRs was chosen to be the same as that of the liquid-phase CSTRs for convenience; this should cause

negligible error for the results reported here due to the depletion being primarily liquid-phase controlled.

Values of k_G and a are calculated from equations from Joshi et al. (12):

$$\frac{k_G R T \ell}{D_i^G} = 0.553 \left\{ \frac{(P_m \ell)^{1/3} \ell \rho_G}{\mu_G} \right\}^{0.62} (Sc)_G^{1/3} \left(\frac{\pi}{P_I} \right), \tag{24}$$

where

$$\ell = 0.25\, d_p , \tag{25}$$

for ceramic Intalox saddles and P_m is the power consumption per unit mass of gas (13):

$$P_m = \frac{f a_p}{6(\varepsilon - \varepsilon_L)^4} G^3 , \tag{26}$$

and

$$a = 19.6\, L^{0.478} d_p^{-1} / \varepsilon^3 . \tag{27}$$

Values of k_L were calculated using a generalized equation from Treybal (14):

$$\frac{k_L d_s}{D^L} = 25.1 \left(\frac{d_s L'}{\mu_L} \right)^{0.45} (Sc)_L^{1/2} . \tag{28}$$

Values of k_1, k_{-1}, and K_1 are from Abel et al. (2, 3, 15). Values of H_{HNO}, H_{NO}, and H_{HNO_3} are from Abel and Neusser (15), Loomis (16), and Hoftyzer and Kwantēn (17), respectively.

The depletion of HNO_2 in the packed column may be found

$$\Phi_T = - \sum_{k=1}^{B} L \, (\Delta C_{HNO_2})_k . \tag{29}$$

Model B

Model B is a simplification of Model A. Simplifying assumptions are: (1) reaction in the liquid mass-transfer film is of negligible importance, (2) the partial pressure of NO in the gas

bulk is of negligible importance to mass transfer, (3) mean driving-force concentrations and partial pressures are adequate for calculating the HNO_2 depletion rates, (4) NO and HNO_2 are the only desorbing species, and (5) the liquid-phase decomposition of HNO_2 is irreversible:

$$-r_{HNO_2} = \frac{k_1}{H_{NO}^2} \frac{C_{HNO_2}^4}{C_{NO}^2} \quad . \tag{30}$$

With the indicated assumptions, the mass-balance equations simplify to:

$$L\Delta C_{HNO_2} = \bar{r}_{HNO_2} \epsilon_L SZ_c + \bar{N}^*_{HNO_2} a SZ_c \quad , \tag{31}$$

and

$$L\Delta C_{NO} = -\frac{2}{3} \bar{r}_{HNO_2} \epsilon_L SZ_c + \bar{N}^*_{NO} a SZ_c \quad . \tag{32}$$

Neglecting the change in concentration of NO in the liquid phase, Eq. (32) becomes:

$$r_{HNO_2} = \frac{3N^*_{NO} a}{2 \epsilon_L} \quad , \tag{33}$$

where

$$N^*_{NO} = K_L \left(\frac{P^o_{NO}}{H_{NO}} - C^o_{NO} \right) = -K_L C^o_{NO} \quad . \tag{34}$$

Combining Eqs. (30), (33), and (34):

$$C^{o\ 3}_{NO} = \frac{2 \epsilon_L k_1 \left(C^o_{HNO_2} \right)^4}{3 K_L a H^2_{NO}} \quad . \tag{35}$$

Substituting this NO concentration into Eq. (30):

$$-r_{HNO_2} = \left(\frac{3}{2} \right)^{2/3} \left(\frac{K_L a}{\epsilon_L} \right)^{2/3} \frac{k_1^{1/3}}{H_{NO}^{2/3}} C_{HNO_2}^{4/3} \quad . \tag{36}$$

Equation (36) applies to packed columns but is mechanically equivalent to Eq. (6). This liquid-phase decomposition of nitrous acid in the column may be found as:

$$\Phi_1 = (-r_{HNO_2})_M \quad \varepsilon_L \, V \, . \tag{37}$$

The desorption flux of nitrous acid may be found as:

$$\Phi_2 = K_L a V \left(\frac{P^\circ_{HNO_2}}{H_{HNO_2}} - C^\circ_{HNO_2} \right)_M \, . \tag{38}$$

A nitrous acid balance around the column yields the total nitrous acid depletion based on the indicated mechanisms:

$$\Phi_T = L(C_{HNO_2,in} - C_{HNO_2,out}) = \Phi_1 + \Phi_2 . \tag{39}$$

EXPERIMENTAL APPARATUS AND PROCEDURE

A flowsheet of the experimental apparatus is shown in Fig. 1. Two packed columns were used with inside diameters (IDs) of 0.076 and 0.102 m. These columns were packed with ceramic Intalox saddles with diameters of 6 and 13 mm, respectively. Runs A through F were conducted using the small-diameter tower, while Run H was conducted using the larger. Other equipment was associated with the scrubber-liquid supply, metering and sampling systems, and the gaseous supply and metering systems. The liquid was recirculated from a holdup tank and distributed in the tower ~0.03 m above the top of the packing.

In these studies, nitrous acid was produced initially by bubbling N_2O_3 through 0.025 m^3 of water in the liquid holdup tank; nitric acid is produced simultaneously by some decomposition of HNO_2. This aqueous solution was then metered continuously to the packed column, where it was contacted with the selected gas. The effluent solution from the column flowed by gravity back to the liquid holdup tank. Recirculation of this solution provided a means of obtaining information on the depletion process(es) over a range of nitrous acid concentrations. The temperature for all runs was approximately 298 K. The 0.076- and 0.104-m-diam towers were operated at 1.1 and 1.4 atmosphere absolute pressure, respectively.

In the 0.076-m-diam column, the gas stream entered into the packing through the packing support; however, the gas was injected directly into the bottom of the packing in the 0.102-m-diam column. Carrier gases of nitrogen, air, or oxygen could be metered by rotameter to either of the two packed towers.

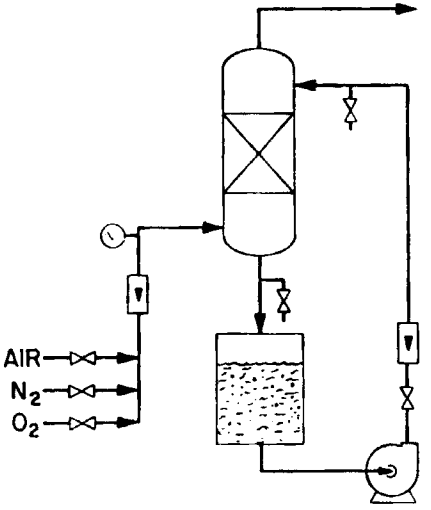

Fig. 1. Schematic drawing of experimental system.

Both feed and effluent liquid samples were stabilized immediately with the addition of excess hydrogen peroxide and ceric sulfate for later analysis of total acid and nitrous acid content. The raw data consisted of gas and liquid flow rates, temperatures and pressures, and the nitrous and acid concentrations in the feed and effluent liquid streams. These data were presented by Counce (18). The entire experimental setup was located in a fume hood.

RESULTS

Two types of analyses are presented. The first deals with the results of varying gas flow rate, liquid flow rate, and column height on the depletion processes; the response variable is the molar ratio of nitric acid produced-to-nitrous acid disappearing, R*. The latter section deals with the application of the previously developed rate expressions to the experimental data.

Effect of G/L Ratio on R*

Specific run conditions are presented in Table 1. The tests described were conducted using a nitrogen feed gas. The quantity, R*, may be determined from the slope of C_{H+} as a function of C_{HNO}. A plot of the data from experiment A is presented as an example in Fig. 2. These concentrations are in the recirculating liquid feed

Table 1. Experimental information

Run	L (m^3/s)	G (std m^3/s)	H (m)
A	1.75×10^{-5}	3.24×10^{-4}	0.15
B	3.50×10^{-5}	3.24×10^{-4}	0.30
C	1.75×10^{-5}	1.57×10^{-4}	0.30
D	3.50×10^{-5}	1.57×10^{-4}	0.15
E	3.60×10^{-5}	1.56×10^{-3}	0.81

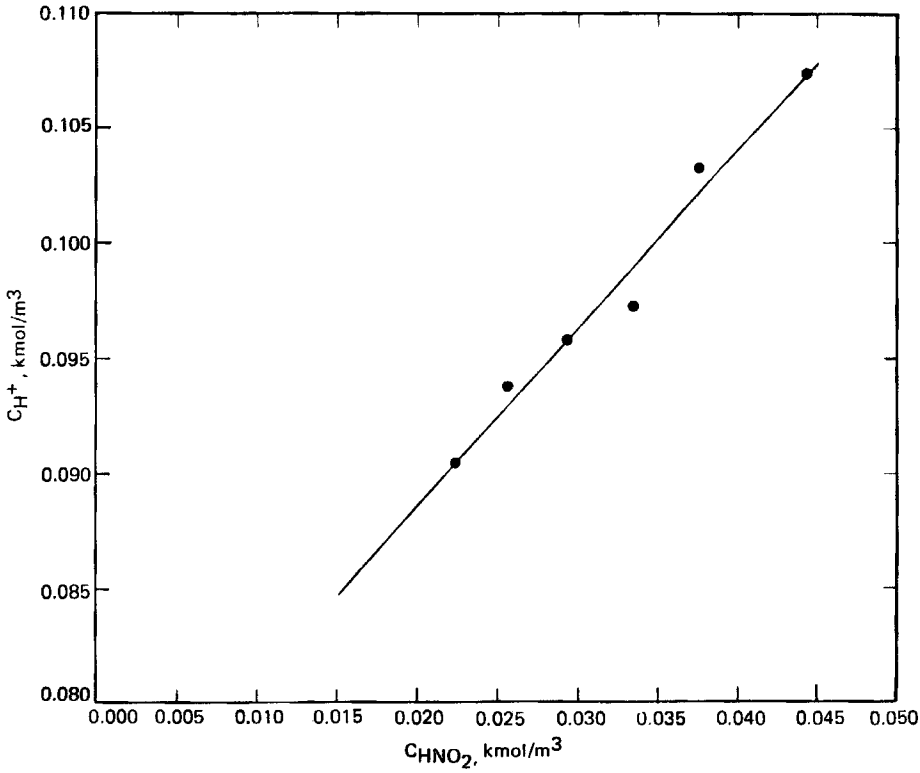

Fig. 2. System total acid concentration as a function of nitrous acid concentration for Experiment A.

Table 2. Variation of experimental R* with G/L ratio

Run	G/L	R*
D	4.5	0.30
C	9.0	0.30
B	9.0	0.28
A	18.5	0.22
H	43.3	0.22

stream to the column; however, they represent the system concentrations at a given time, assuming that the liquid holdup tank is well mixed. This type of analysis was used because the change in acid concentrations in a single pass through the column was small and the resultant R* results were scattered. There appears to be a systematic decrease in the value of R* with increasing G/L ratios in these experiments as shown in Table 2. This may be explained with liquid-phase decomposition, which produces an R* of 0.33 being kinetic and mass-transfer limited while nitrous acid in the liquid phase remains at near equilibrium with the species in the gas phase.

COMPARISON OF MODEL AND EXPERIMENTAL DATA

Analysis of Depletion Rate

The values of R* indicate that liquid-phase decomposition is largely responsible for the nitrous acid depletion at lower gas rates. The values of R* from the tests at higher gas rates indicate that both liquid-phase decomposition and direct desorption are occurring to substantial extent. Overall, the ratio of gas-to-liquid rates was observed to effect the depletion stoichiometry as found by previous researchers.

Both Model A and Model B predict that the value of R* decreases as the concentration of nitrous acid decreases for every experiment. The ranges of the values of R* predicted by the two models for these experiments are compared to the average experimental R*s in Table 3; the predicted values of R* are within the 95% confidence intervals also shown in this Table 3.

Table 3. R* predicted by the two models

Run	Range for Model A	Range for Model B	Experimental mean value	95% confidence interval
A	0.221, 0.232	0.236, 0.249	0.22	0.05, 0.39
B	0.283, 0.297	0.290, 0.304	0.28	0.18, 0.39
C	0.294, 0.303	0.300, 0.309	0.30	0.25, 0.35
D	0.281, 0.289	0.297, 0.304	0.30	0.21, 0.39
H	0.236, 0.272	0.205, 0.258	0.22	0.17, 0.28

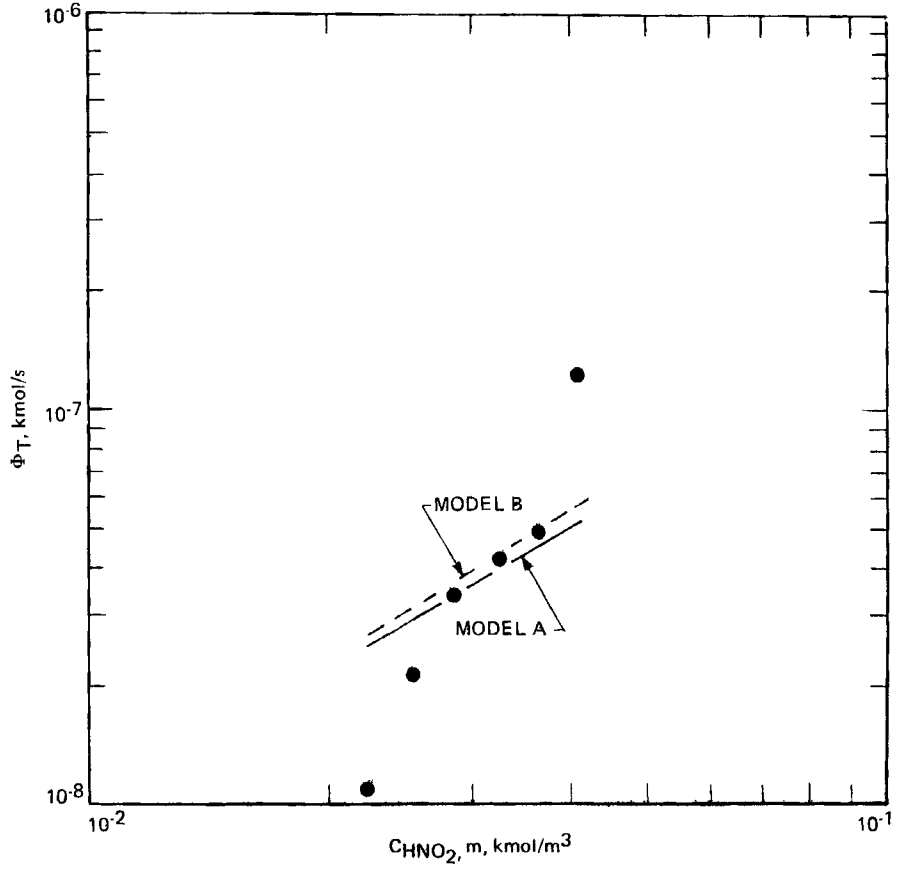

Fig. 3. Predictions from Models A and B vs experimental data for Experiment A.

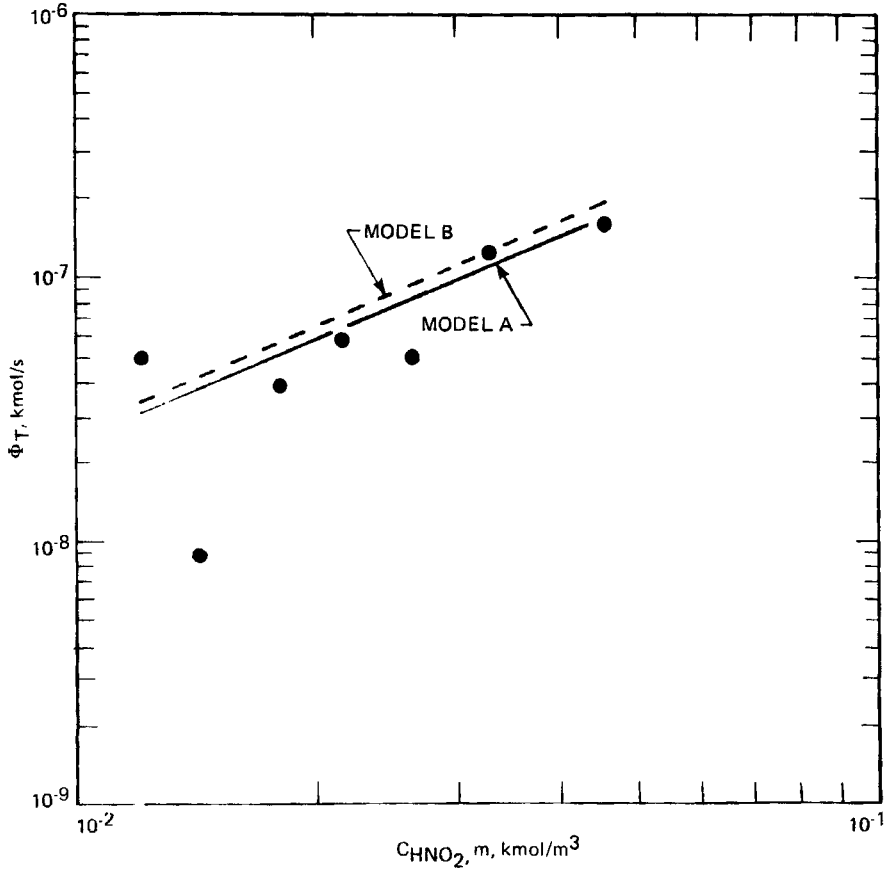

Fig. 4. Predictions from Models A and B vs experimental data for Experiment B.

The experimental depletion rate results are compared with the results predicted by the two models in Figs. 3 through 6 for the depletion of nitrous acid in the smaller diameter tower. Using estimates from correlations of k_L, k_G, a, and ϵ_L (12, 13, 19), the depletion rates predicted by both models A and B are within the scatter of the experimental data.

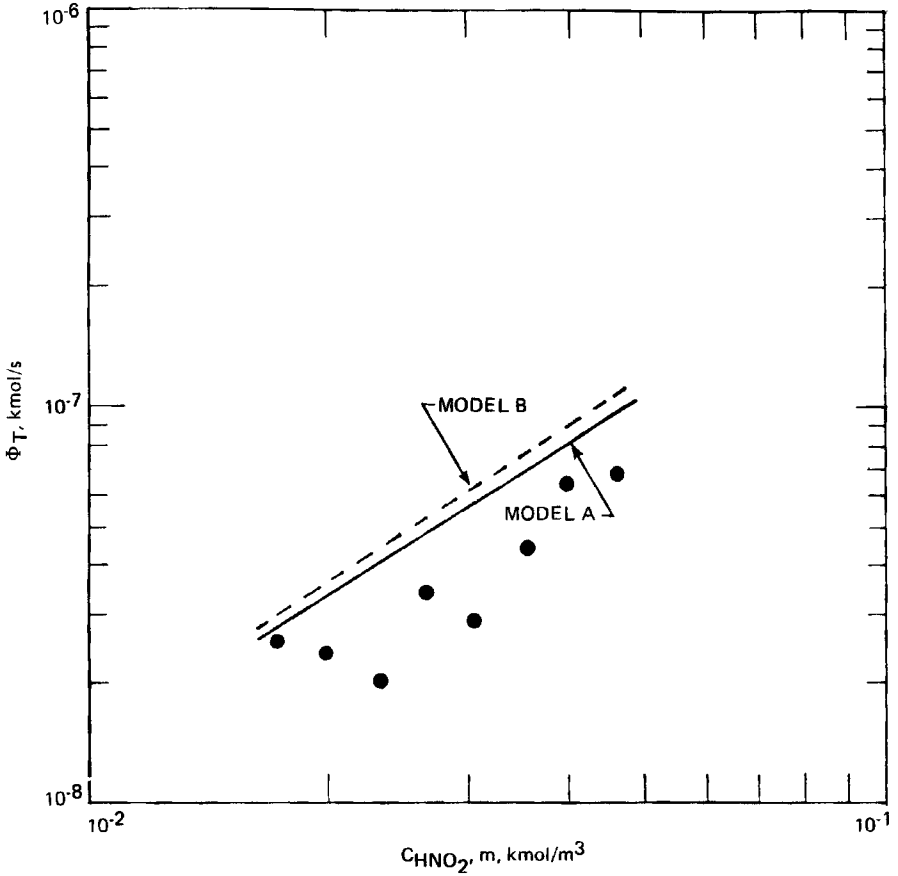

Fig. 5. Predictions from Models A and B vs experimental data for Experiment C.

Experiment H is unique among the experiments because it is the only experiment using the large diameter tower. Moreover, only Experiment H has data for the partial pressure of nitric oxide leaving the column. Figure 7 shows that both models are in reasonable agreement with the experimental depletion rate data. However, in Fig. 8, it is apparent that predictions from model B are slightly better in agreement with the experimental data. Both

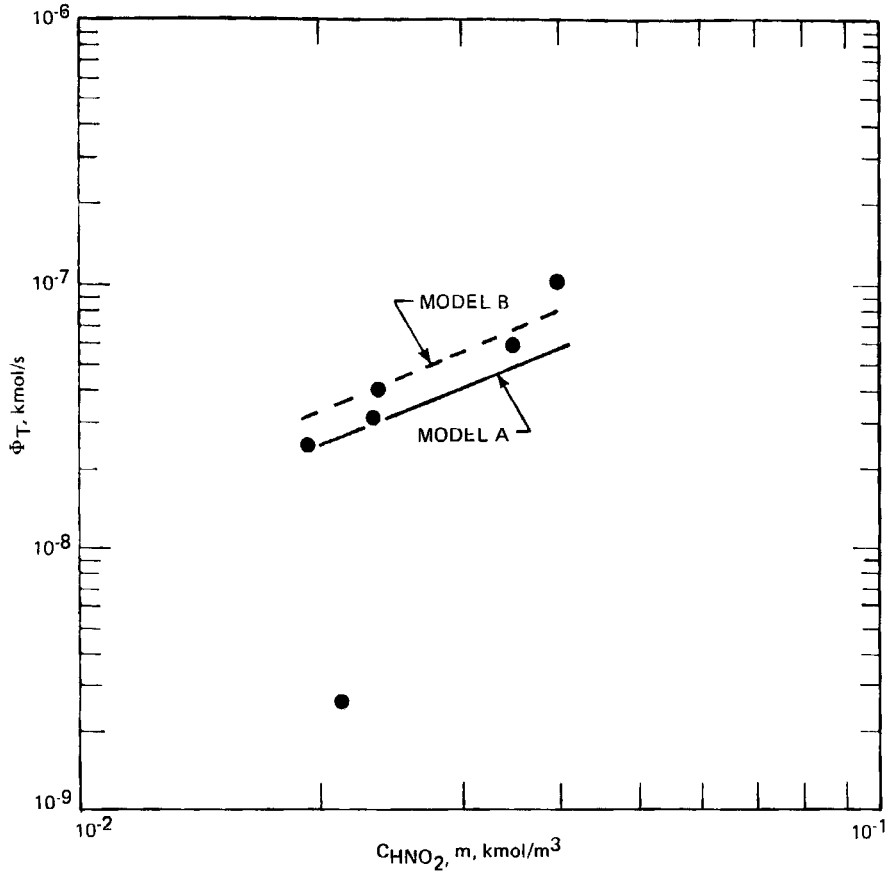

Fig. 6. Predictions from Models A and B vs experimental data for Experiment D.

models represent the experimental data very well; the use of a generalized correlation for k_L adds sufficient uncertainty to make further discrimination between models A and B of little benefit. Overall, the similarity of the depletion-rate prediction of both models indicate that the liquid-phase depletion of HNO_2 occurs primarily in the bulk-liquid phase for the conditions studied.

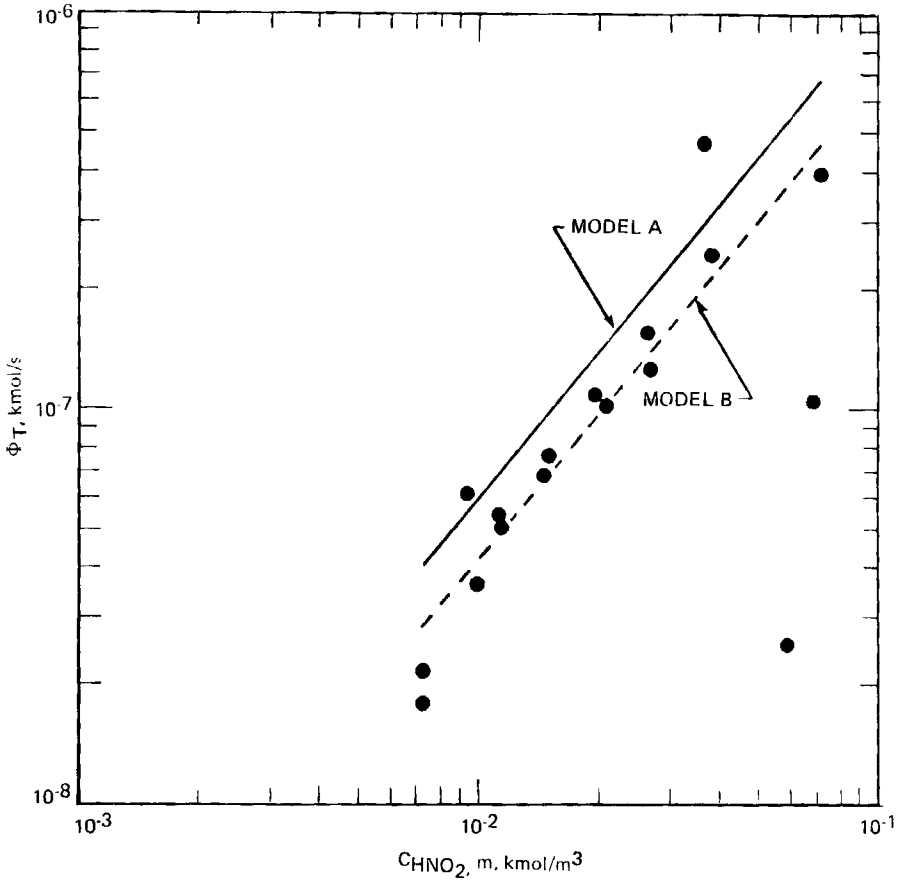

Fig. 7. Predictions from Models A and B vs experimental data for Experiment H.

CONCLUSIONS

The results indicate the existence of two primary depletion mechanisms: liquid decomposition and direct desorption of HNO_2. Both models A and B provide quite similar predictions which indicate that the liquid-phase decomposition occurs primarily in the bulk-liquid region, with little occurrence in the liquid-phase mass-transfer film. These results are in agreement with the approach used by Counce and Perona (1) to model the depletion of

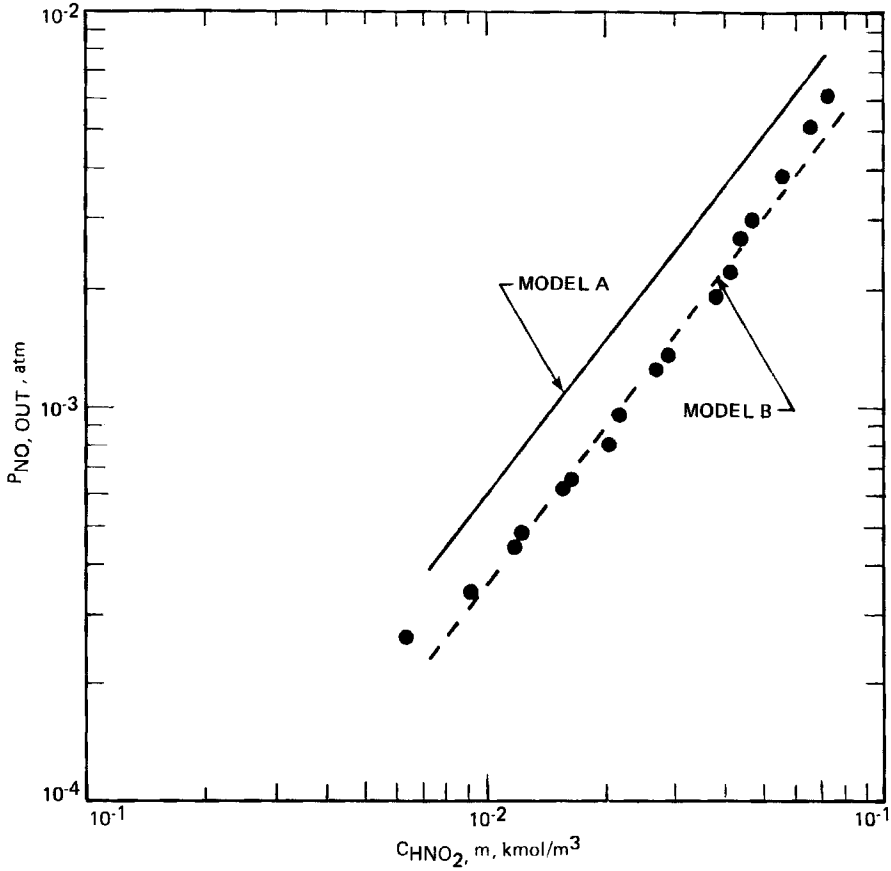

Fig. 8. Predictions of effluent partial pressure of NO from Models A and B vs experimental data for Experiment H.

HNO_2 that occurs during NO_x scrubbing; their HNO_2 depletion model was very similar to model B. These results should also be useful for further NO_x scrubber modeling and simulation of processes for the removal of HNO_2 from aqueous solutions.

NOMENCLATURE

a	gas-liquid interfacial area based upon total column volume, m^2/m^3

a'	gas-liquid interfacial area based upon liquid volume, m^2/m^3
a_p	dry surface area of the packing, m^2/m^3
B	number of CSTRs-in-series
C_i	concentration of component i, $kmol/m^3$
C_i^*	concentration of component i at the gas-liquid interface, $kmol/m^3$
C_i^o	concentration of component i in the liquid bulk, $kmol/m^3$
C_T	total molar concentration of the liquid phase, $kmol/m^3$
D_i^G	binary diffusivity of component i in gaseous N_2, m^2/s
D_i^L	binary diffusivity of component i in liquid H_2O, m^2/s
D_i	binary diffusivity of component i in gaseous component j, m^2/s
d_p	nominal diameter of the packing, m
d_s	diameter of a sphere with the same surface area of a piece of the packing, m
f	friction factor for the packing
G	volumetric flow rate of the gas, m^3/s
Ga	Gallileo number
(g)	denotes a component in the gas phase
H_i	Henry's Law constant for component i, m^3 atm/kmol
K_1	equilibrium constant for reaction (1), $atm^2m^3/kmol$
k_1	forward rate constant for reaction (1), $atm^2{}_m{}^g/kmol^3{}_s$
k_{-1}	reverse rate constant for reaction (1), $m^6/kmol^2s$
k_G	gas-phase mass-transfer coefficient, $kmol/m^2$ atm s
K_i	gas-liquid equilibrium constant for component i, m^3 atm/kmol
K_L	overall liquid-phase mass transfer coefficient, m/s

k_L	liquid-phase mass-transfer coefficient, m/s
L	liquid volumetric flow rate, m^3/s
L'	superficial mass velocity of liquid phase, kg/m^2s
ℓ	packing parameter for Eqs. (24) and (25), m
(ℓ)	denotes a component in the liquid phase
N_i	molar flux of component i, $kmol/m^2s$
N_{i*}	molar flux of component i at the gas-liquid interface, $kmol/m^2s$
P_i	partial pressure of component i, atm
P_{i*}	partial pressure of component i at the gas-liquid interface, atm
P_m	power consumption per unit mass of the gas, N m/kg
Pe	Peclet number
R	ideal gas low constant, m^3 atm/kmol K
R*	ratio of moles of nitric acid produced-to-moles of nitrous acid disappearing
Re	Reynolds number
$-r_{HNO}$	rate of disappearance of nitrous acid by reaction (1), $kmol/m^3s$
S	cross-sectional area of the column, m^2
Sc	Schmidt number
T	temperature, K
V	volume of the column, m^3
X	distance through the film, m
Z	distance up the column, m
Z_c	height of the column, m

Greek Letters

Δ	denotes an increment
Φ_1	rate of depletion of nitrous acid by reaction (1), kmol/s
Φ_2	rate of depletion of nitrous acid by direct desorption, kmol/s
Φ_T	total depletion rate of nitrous acid, kmol/s
δ_G	gas-phase film thickness, m
δ_L	liquid-phase film thickness, m
ϵ	column void fraction
ϵ_L	liquid holdup fraction
μ	viscosity, kg/m s
ν_i	stoichimetric coefficient of component i
π	total pressure, atm
ρ	density, kg/m^3

ACKNOWLEDGEMENT

The experimental portion of this work was performed in the Fuel Recycle Division under the auspices of the Consolidated Fuel Reprocessing Program of the Oak Ridge National Laboratory and was sponsored by the U.S. Department of Energy under contract DE-AC05-84OR2140 with Martin Marietta Energy Systems, Inc. The analytical portion of the work was sponsored by the State of Tennessee Center of Excellence for Waste Management. T. L. Hebble of the Engineering Physics and Mathematics Division at the Oak Ridge National Laboratory provided much of the statistical elements of this work.

REFERENCES

1. Counce, R. M., and J. J. Perona, "The Scrubbing of Gaseous Nitrogen Oxides in Packed Towers," AIChE J. (1983).

2. Abel, E., and H. Schmid, "Kinetics of Nitrous Acid I: Introduction and Survey," Z. Phys. Chem. 132, 55 (1928), translated from German (ORNL-tr-4263).

3. Abel, E., and H. Schmid, "Kinetics of Nitrous Acid III: Kinetics of the Decomposition of Nitrous Acid," Z. Phys. Chem. 134, 279 (1928), translated from German (ORNL-tr-4264).

4. Andrews, S. P. S., and D. Hanson, "The Dynamics of Nitrous Gas Absorption," Chem. Eng. Sci. 14, 105 (1961).

5. Komiyama, H., and H. Inoue, "Absorption of Nitrogen Oxides into Water," Chem. Eng. Sci. 35, 154 (1978).

6. Lang, F. M., and G. Aunis, "Rate of Change in Nitrous Acid in Aqueous Solution I. – Evolution in Open Air, Bull. Soc. Chem. de France 18(5), 135 (1951).

7. Lang, F. M., and G. Aunis, "Rate of Change in Nitrous Acid in Aqueous Solution II. – Evolution in Various Gaseous Atmospheres," Bull. Soc. Chem. de France 18(5), 398 (1951).

8. Safin, R. S., A. F. Mokhotkin, and A. F. Galeev, "Experimental Study of the Kinetics of Nitrous Acid Desorption from Aqueous Solution," Sb. Aspir. Rab. Kazan. Khim. Tekhnol. Inst. Khim. Nauk. 1, 166 (1970).

9. Liebmann, H., Beitrage zur kinntnis der sapetrigen saure, Ph.D., dissertation, University of Dresden, Germany (1914).

10. Carberry, J. J., Chemical and Catalytic Reaction Engineering, McGraw-Hill, New York 1976.

11. Otake, T., and E. Kunugita, Chem. Eng. (Japan) 22, 144 (1958).

12. Joshi, J. B., V. V. Mahajami, and V. A. Juvekar, "Absorption of NO_x Gases," Chem. Eng. Commun. 33, 1 (1985).

13. Niranjun, K., V. G. Pargarkar, and J. G. Joshi, "Estimate Tower Pressure Drop," Chemical Engineering, ?, 67 (1983).

14. Treybal, R. E., Mass Transfer Operations, 3rd Ed., McGraw-Hill, New York, 1980.

15. Abel, E., and E. Neusser, Monatsh. Chem. 54, 855 (1929).

16. Loomis, A. G., "Solubilities of Gases in Water," International Critical Tables 3, McGraw-Hill, New York, 1928, p. 581.

17. Hoftyzer, P. J., and F. J. G. Kwanten, Processes for Air Pollution Control, 2nd Edition, Chemical Rubber Co., Cleveland (1972).

18. Counce, R. M., "The Scrubbing of Gaseous Nitrogen Oxides in Packed Towers," Ph.D. dissertations, The University of Tennessee, Knoxville, 1980.

19. Sater, V. E., and O. Levenspiel, "Two-Phase Flow in Packed Beds," Ind. Eng. Chem. Fundam. 5, 86 (1956).